Capture and purification of Human Immunodeficiency Virus-1 virus-like particles: Convective media vs porous beads

Patricia Pereira Aguilar, Katrin Reiter, Viktoria Wetter, Petra Steppert, Daniel Maresch, Wai Li Ling, Peter Satzer, Alois Jungbauer

Journal of Chromatography A 1627 (2020) 461378

Contents lists available at ScienceDirect

Journal of Chromatography A

journal homepage: www.elsevier.com/locate/chroma

Capture and purification of Human Immunodeficiency Virus-1 virus-like particles: Convective media vs porous beads

Patricia Pereira Aguilar[a,b], Katrin Reiter[b], Viktoria Wetter[b], Petra Steppert[a], Daniel Maresch[a], Wai Li Ling[c], Peter Satzer[b,*], Alois Jungbauer[a,b]

[a] Department of Biotechnology, University of Natural Resources and Life Sciences, Vienna, Austria
[b] Austrian Centre of Industrial Biotechnology, Vienna, Austria
[c] Univ. Grenoble Alpes, CEA, CNRS, IBS, F-38000 Grenoble, France

ARTICLE INFO

Article history:
Received 20 December 2019
Revised 24 June 2020
Accepted 28 June 2020
Available online 9 July 2020

Keywords:
Enveloped VLP
Affinity chromatography
Ion exchange chromatography
Polymer-grafted media
Convective media
Downstream processing

ABSTRACT

Downstream processing (DSP) of large bionanoparticles is still a challenge. The present study aims to systematically compare some of the most commonly used DSP strategies for capture and purification of enveloped viruses and virus-like particles (eVLPs) by using the same staring material and analytical tools. As a model, Human Immunodeficiency Virus-1 (HIV-1) gag VLPs produced in CHO cells were used. Four different DSP strategies were tested. An anion-exchange monolith and a membrane adsorber, for direct capture and purification of eVLPs, and a polymer-grafted anion-exchange resin and a heparin-affinity resin for eVLP purification after a first flow-through step to remove small impurities. All tested strategies were suitable for capture and purification of eVLPs. The performance of the different strategies was evaluated regarding its binding capacity, ability to separate different particle populations and product purity. The highest binding capacity regarding total particles was obtained using the anion exchange membrane adsorber (5.3×10^{12} part/mL membrane), however this method did not allow the separation of different particle populations. Despite having a lower binding capacity (1.5×10^{11} part/mL column) and requiring a pre-processing step with flow-through chromatography, Heparin-affinity chromatography showed the best performance regarding separation of different particle populations, allowing not only the separation of HIV-1 gag VLPs from host cell derived bionanoparticles but also from chromatin. This work additionally shows the importance of thorough sample characterization combining several biochemical and biophysical methods in eVLP DSP.

1. Introduction

The growing interest in the use of enveloped virus-like particles (eVLPs) as novel vaccines or vectors for gene and cancer therapy applications lead to an increase demand for efficient and scalable production platforms [1-3]. Current downstream processing (DSP) strategies in eVLP production still rely on the combination of several sub-optimal unit operations, including ultracentrifugation, filtration and chromatography [4-6]. Here we compare different DSP strategies for eVLP purification including the use of monoliths, membrane adsorbers, polymer-grafted media and core-shell beads. Drawbacks of the combination of several sub-optimal unit operations in a DSP strategy include long process times, low productivity and high product losses. Furthermore, the lack of standard methods for detection and quantification of eVLPs leads to the use of methodologies imported from protein biotechnology, which are non-optimal for eVLPs, consequently hindering process development and optimization [2,7]. Besides that, the use of protein-based methods for quantification of specific proteins of different eVLPs makes a systematic comparison between the currently available eVLP DSP strategies unfeasible. In this work, we compared the performance of four different chromatography-based DSP strategies for capture and purification of a model eVLP, using the same starting material. Several works have shown that anion-exchange chromatography allows the efficient capture and purification of enveloped viruses and VLPs [8-11]. Monoliths and membrane adsorbers are attractive options as unit operation for bionanoparticle's DSP due to their convective flow properties and large surface area accessible for binding of large molecules [12-14]. Several enveloped viruses and VLPs have been purified using anion-exchange mono-

* Corresponding author at: Dipl.Ing Peter Satzer, Ph.D, Austrian Centre of Industrial Biotechnology, Vienna, Austria, Muthgasse 18, 1190 Vienna.
E-mail address: peter.satzer@boku.ac.at (P. Satzer).

https://doi.org/10.1016/j.chroma.2020.461378

liths, such as baculoviruses, different influenza virus A and B subtypes and HIV-1 gag VLPs [15-17]. Also, membrane adsorbers have been successfully used for the capture and purification of baculovirus and influenza viruses, among others [18-20]. In contrast to convective media, in porous-bead based chromatography, mass transfer mainly occurs through pore diffusion and pores are usually too small to allow VLP diffusion into the pores. Nevertheless, it was shown that even when eVLPs are completely excluded from the resin's pores, the bead's outer surface area still provides satisfactory binding capacity, which is only one order of magnitude smaller than the one obtained with convective media [8]. Moreover, the scalability of conventional chromatography resins easily overcomes its lower biding capacity as current monolith technology is limited in column size to a couple liters. Accordingly, we selected three different types of anion exchangers: a monolithic support, a membrane absorber and a polymer-grafted bead resin. Besides anion-exchange chromatography, affinity chromatography has great potential for capture and purification of eVLPs, once it allows the direct capture of the product of interest from complex feed streams, resulting in high levels of purity in a single step [4]. This increases DSP productivity and accelerates R&D. Since heparin is a natural cell receptor for many viruses [21] and it was already reported that heparin-affinity can separate eVLPs from host cell derived bionanoparticles [22], we selected a heparin-affinity resin. However, due to the possible presence of heparin-binding proteins in the cell culture supernatant, a first pre-processing step is required to avoid reduction in binding capacity or co-elution of protein impurities with the eVLP product. For that purpose, we use flow-through chromatography with core-shell beads in which the VLPs flow-through the column without reaching the active core of the beads where the proteins can bind [23,24]. As model eVLP, we used HIV-1 gag VLPs (100-200 nm in diameter) produced in Chinese Hamster ovary (CHO) cells. Structurally VLPs mimic their native viruses, resulting in complex bionanoparticles containing several copies of one or more viral proteins. These proteins typically self-assemble in spherical-like structures with sizes ranging from tens to hundreds of nanometers in diameter. In the case of eVLPs, as for enveloped viruses, an additional lipid bi-layer composed of the host cell membrane is part of their structure [7,25]. These complex structural features of eVLPs bring new challenges to the production platforms. Efficient DSP development requires fast and high-resolution analytical methods for in-process product quality and quantity control. However, there are no methods which allow the direct quantification of eVLPs in complex mixtures. Consequently, eVLP titers are often measured based on the quantification of a single viral protein or total particle count, which leads to under- or over-estimated titers [5,26,27]. Detection and quantification methods based on infectivity assays are not applicable for VLPs once they lack viral genome and are therefore non-infectious. Especially in DSP development and analytics additional challenges arise from the simultaneous release of host cell derived nanoparticles, such as exosomes and extracellular vesicles, which have similar structure, size and composition as the eVLPs [28]. Besides that, dsDNA is another challenging impurity due to its overall negative charge, which is similar to the charge of many enveloped viruses and VLPs [29]. Especially when using anion-exchange based methods, co-elution of eVLPs and dsDNA was observed [8,9]. Accordingly, we used a combination of several biochemical and biophysical analytical methods to detect, quantify and characterize particle populations, including multi-angle light scattering (MALS), nanoparticle tracking analysis (NTA), cryo transmission electron microscopy (cryo-TEM), Western blot analysis and mass spectrometry (MS). The use of the same analytical methodologies to access product quantity and quality as well as the use of the same starting material, allowed a systematic comparison of the binding capacity and resolution for particle separation of an anion-exchange monolith, a membrane adsorber, a polymer-grafted anion-exchange resin and a heparin-affinity resin.

2. Material and methods

2.1. Chemicals and standards

All chemicals were acquired from Sigma Aldrich (St. Louis, MO, USA), Merck (Darmstadt, Germany) or Abcam (Cambridge, England) and were of analytical grade, if not otherwise stated.

2.2. Enveloped VLP production

HIV-1 gag VLPs, kindly provided by Icosagen (Tartumaa, Estonia), were used as an enveloped VLP model. VLP production was carried out in CHOEBNALT85 cells using a stable episomal system as described by Steppert *et al* [9]. Cell culture was harvested by centrifugation (1000 g, 30 min) and 0.01% NaN_3 was added to the supernatant.

2.3. Endonuclease treatment

Benzonase® purity grade II (Merck KGaA, Darmstadt, Germany) was used for the digestion of double stranded DNA (dsDNA). The digestion was performed by incubating cell culture supernatant with 150 U/mL Benzonase® and 2 mM $MgCl_2$ for 2 h at 37°C.

2.4. Preparative chromatography

2.4.1. Chromatographic system

All chromatographic experiments were performed on an Äkta pure 25 M2 equipped with a 1.4 mL mixer chamber, a S9 sample pump and a F9-C fraction collector (GE Healthcare, Uppsala, Sweden). System control and data acquisition were performed using the Unicorn 6.4.1 software. UV absorbance (280, 260 and 214 nm) and conductivity were continuously monitored.

2.4.2. Chromatography media and mobile phases

All preparative chromatographic experiments for capture and purification of eVLPs were performed using 50 mM HEPES, pH 7.2 as mobile phase A and 50 mM HEPES, 2 M NaCl, pH 7.2 as mobile phase B. Different concentrations of the modifier were obtained by mixing mobile phases A and B using the chromatography system. If not further stated, cleaning in place was performed using 0.5 M NaOH solution. The used chromatography media are summarized in Table 1. All materials were used for a single cycle.

2.4.3. Capture and purification of HIV-1 gag VLPs

For the capture and purification of HIV-1 gag VLPs, clarified CHO cell culture supernatant was endonuclease treated and either directly loaded onto the column or pre-processed using flow-through chromatography (Capto-Core). Direct loading was used for Natrix-Membrane and QA-Monolith devices. Fractogel-TMAE and Capto-Heparin columns were loaded with the flow-through fractions of the pre-processing runs. For the packed columns (Fractogel-TMAE and Capto-Heparin) flow rates were defined in order to achieve a 5 min residence time. For the pre-packed devices (Natrix-Membrane and QA-Monolith) flow rates recommended by the manufacturers were used. In all chromatographic experiments, equilibration of the stationary phase was performed before loading using equilibration buffer (50 mM HEPES, 100 mM NaCl, pH 7.2 / 5% B). After loading, columns were washed with equilibration buffer to ensure the removal of unbound material from the column. In the capture and purification experiments, elution was achieved by salt linear gradients. Details of flow rates, loading volumes and elution gradients are summarized in Table 2. After the

Table 1
Chromatography media used for preparative chromatography.

Type of chromatography		Name	Referred in the text as	Manufacturer	Column volume (mL)
Anion exchange	Membrane adsorber / hydrogel (porous polyacrylamide)	NatriFlo® HD-Q Recon	Natrix-Membrane	Merck, Darmstadt, Germany	0.8
	Poly-methacrylate based monolithic column	CIMmultus™ QA-8 2 µm	QA-Monolith	BIA Separations, Ajdovščina, Slovenia	8.0
	Methacrylate based polymer grafted beads	Fractogel® EMD TMAE Hicap (M)	Fractogel-TMAE	Merck, Darmstadt, Germany	23.0
Affinity (Heparin)	Agarose based beads	Capto™ Heparin	Capto-Heparin	GE Healthcare, Uppsala, Sweden	22.0
Flow-through	Agarose based core beads	Capto™ Core 700	Capto-Core	GE Healthcare, Uppsala, Sweden	50.4

Table 2
Flow rates, loading volumes and elution gradients of chromatographic experiments.

Run code	Chromatography media	Flow rate (mL/min)	Residence time (min)	Loading volume (mL)	Linear gradient elution
1902-NT	NatriFlo® HD-Q Recon	4.0	0.2	95	5 – 75% B in 75 CV (60 mL)
1904-CH	Capto™ Heparin	4.4	5.0	212	5 – 75% B in 4 CV (88 mL)
1903-CC	Capto™ Core 700	10.0	5.0	350	n.a.
1905-M	CIMmultus™ QA-8 2 µm	8.0	1.0	450	5 – 60% B in 30 CV (240 mL)
1906-CC	Capto™ Core 700	10.0	5.0	450	n.a.
1907-FG	Fractogel® EMD TMAE Hicap (M)	4.6	5.0	400	5 – 60% B in 15 CV (345 mL)

elution phase, columns were regenerated using 100% B buffer. Fractions were collected and pooled according to the chromatograms, considering both, the light scattering intensity and the UV absorbance signals.

2.5. Particle detection and quantification

Particle detection of collected fractions from the chromatographic experiments was performed by at-line multi-angle light scattering (MALS) measurements as described in [30]. Briefly, an Ultimate 3000 system (Thermo Fisher, Waltham, MA, USA) was used in bypass mode for the direct injection of each collected fraction into the MALS detector (DAWN HELEOS 18-angle, Wyatt, Santa Barbara, CA, USA). The peak area of the light scattering signal measured at 90° angle was used to access the light scattering intensity which is proportional to the particle concentration. This information together with the UV data was used to decide on sample pooling.

Particle concentration of pooled samples was accessed by nanoparticle tracking analysis (NTA) using a NanoSight NS300 (Malvern Instruments Ltd., Worcestershire, UK) equipped with a blue laser module (488 nm). For the NTA measurements, samples were diluted using particle-free water in order to achieve a concentration of 20 to 80 particles per video frame (equivalent to 1×10^8 to 5×10^8 part/mL). For each sample, 3 dilutions were measured, and 5 videos were recorded for each dilution. In total 15 videos of 30 seconds were recorded per sample. NanoSight NTA software version 3.2 (Malvern Instruments Ltd., Worcestershire, UK) was used to record and analyse the data.

Transmission electron microscopy (TEM) was used to visualize the structure of the particles in relevant samples. Negative staining was used to prepare grids with native or antibody labelled samples. For native samples, 30 µL of sample were incubated on coated 400-mesh copper grids for 1 min at room temperature. Fixation was performed by incubating the grids in 2.5% glutaraldehyde solution (in 100 mM cacodylate buffer, pH 7.0) for 15 min. Finally, grids were stained with 1% uranyl acetate for 30 seconds. Specimens were visualized using a Tecnai G2 200 kV transmission electron microscope (FEI, Eindhoven, The Netherlands). For cryo-TEM, 4 µL of the sample were applied to a glow-discharged holey carbon grid and plunge frozen in liquid ethane using a FEI Vitrobot™ mark IV (ThermoFisher Scientific, Oregon, USA). Imaging was performed on an FEI F20 microscope at 200 kV and recorded on an FEI Ceta detector (ThermoFisher Scientific, Oregon, USA). For TEM and cryo-TEM undiluted samples were used.

2.6. Protein and DNA detection and quantification

Total protein was quantified by Bradford assay using Coomassie blue G-250-based protein dye reagent (Bio-Rad Laboratories, Hercules, CA, USA). Double stranded DNA (dsDNA) was quantified by Quant-iT™ PicoGreen® dsDNA kit (Life Technologies, Waltham, MA, USA). Both quantifications were performed according to the manufacturer's instructions in a microtiter plate format.

Total protein content was also qualitatively evaluated by sodium dodecyl sulphate polyacrylamide gel electrophoresis (SDS-PAGE) as described in [8]. Specific proteins (HIV-1 gag p24 and H3 histone) were detected by Western blot analysis as described in [8].

Proteomic analysis using mass spectrometry was performed for protein identification. For that purpose, relevant samples were digested in solution. Proteins were S-alkylated with iodoacetamide and digested with Trypsin (Promega, Madison, WI, USA). Digested samples were analysed as described before in [8].

2.7. Analytical chromatography

Size exclusion chromatography coupled to multi-angle light scattering (SEC-MALS) was used to access sample composition and purity. An Ultimate 3000 HPLC system (Thermo Fisher, Waltham, MA, USA) with a quaternary LPG-3400SD pump, a WPS-3000TSL autosampler and a DAD 3000 UV-detector was used as chromatography system. A TSKgel G5000PWxl 30.0 cm × 7.8 mm i.d. column in combination with a TSKgel PWxl guard column 4.0 cm × 6.0 mm i.d. or a TSKgel SuperMultiporePW-H 15.0 cm × 6.0 mm column (Tosoh Bioscience, Stuttgart, Germany) were used as SEC columns. A DAWN HELEOS 18-angle (Wyatt, Santa Barbara, CA, USA) was used as multi-angle light scattering detector. Mobile phase consisted of 50 mM HEPES, 100 mM NaCl, pH 7.2. Flow rate was 0.3 mL/min for the G5000PWxl column and 0.175 mL for the SupermultiporePW-H column. In both cases, sample volume was 50 µL. HPLC was controlled by Chromeleon 7 software (Thermo Fisher, Waltham, MA, USA). MALS data collection and analysis was performed with ASTRA software, version 6.1.2 (Wyatt, Santa Barbara, CA, USA).

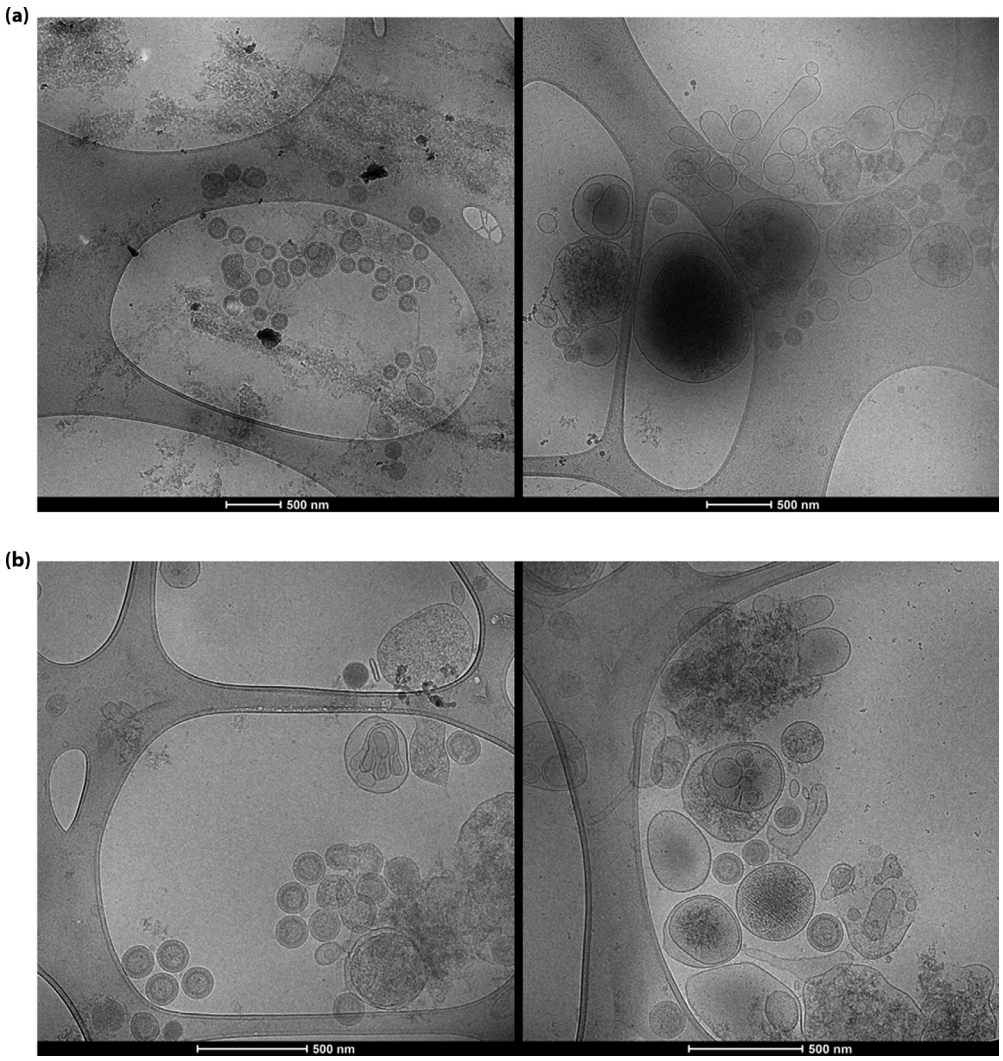

Fig. 1. Cryo-TEM micrographs showing HIV-1 gag VLPs and several host cell derived particles from (a) endonuclease treated and 0.8 µm filtered CHO cell culture supernatant used for the capture and purification experiments with the NatriFlo® HD-Q Recon membrane adsorber or the CIMmultus™ QA-8 monolith; (b) collected flow-through from the pre-processing experiments with Capto™ Core 700, later used for the capture and purification experiments using Fractogel® EMD TMAE Hicap (M) or Capto™ Heparin media.

3. Results and discussion

3.1. Feed material composition before and after pre-processing

After clarification by centrifugation, CHO cell culture supernatant contained approximately 1×10^{11} part/mL, 830 µg/mL of total protein and 22 µg/mL of dsDNA, determined by NTA, Bradford assay and Picogreen assay, respectively. Cryo-electron microscopy revealed the presence of several enveloped bionanoparticle populations including HIV-1 gag VLPs and host cell derived vesicles such as microvesicles and exosomes (Fig. 1a). To be used as feed material for direct loading of anion-exchange monoliths and membrane adsorbers, clarified CHO cell culture supernatant was endonuclease pre-treated and 0.8 µm filtered. Resulting feed material contained approximately 1×10^{11} part/mL, 800 µg/mL of total protein and 0.5 µg/mL of dsDNA (98% reduction in dsDNA content). To be suited as feed material for the heparin-affinity resin, endonuclease pre-treated and 0.8 µm filtered CHO cell culture supernatant was further pre-processed by flow-through chromatography. For that purpose, a HiScale 26/20 column packed with 50.4 mL of Capto-Core resin was used. A recovery of approximately 82% of particles with a reduction of 76% in total protein and 34% in dsDNA was obtained (Supplementary material A, Figures SA1 and SA2) during the pre-processing of the feed material for the heparin-affinity experiment. Similar results were obtained while preparing the feed material for the polymer-grafted anion-exchanger. While the pre-processing with flow-through chromatography allowed the reduction of host cell protein and dsDNA content, removal of host cell derived bionanoparticles was not possible using this method (Fig. 1b). Further purification of this material was done using heparin-affinity and anion-exchange chromatography.

3.2. Binding capacity

When using cell culture supernatant as feed material (with or without pre-processing), it is not possible to accurately determine the concentration of HIV-1 gag VLPs due to the presence of other bionanoparticles and the lack of specific analytical methods to quantify eVLPs in these complex mixtures. Subsequently, it is no possible to determine the dynamic binding capacity for the HIV-1 gag VLPs directly. However, since it was possible to identify the particle breakthrough by the light scattering signal (Fig. 2, LS area) we used this signal to estimate the binding capacity for all bionanoparticles in general. For comparison reasons, the estimation of the binding capacity was done considering the loading volume

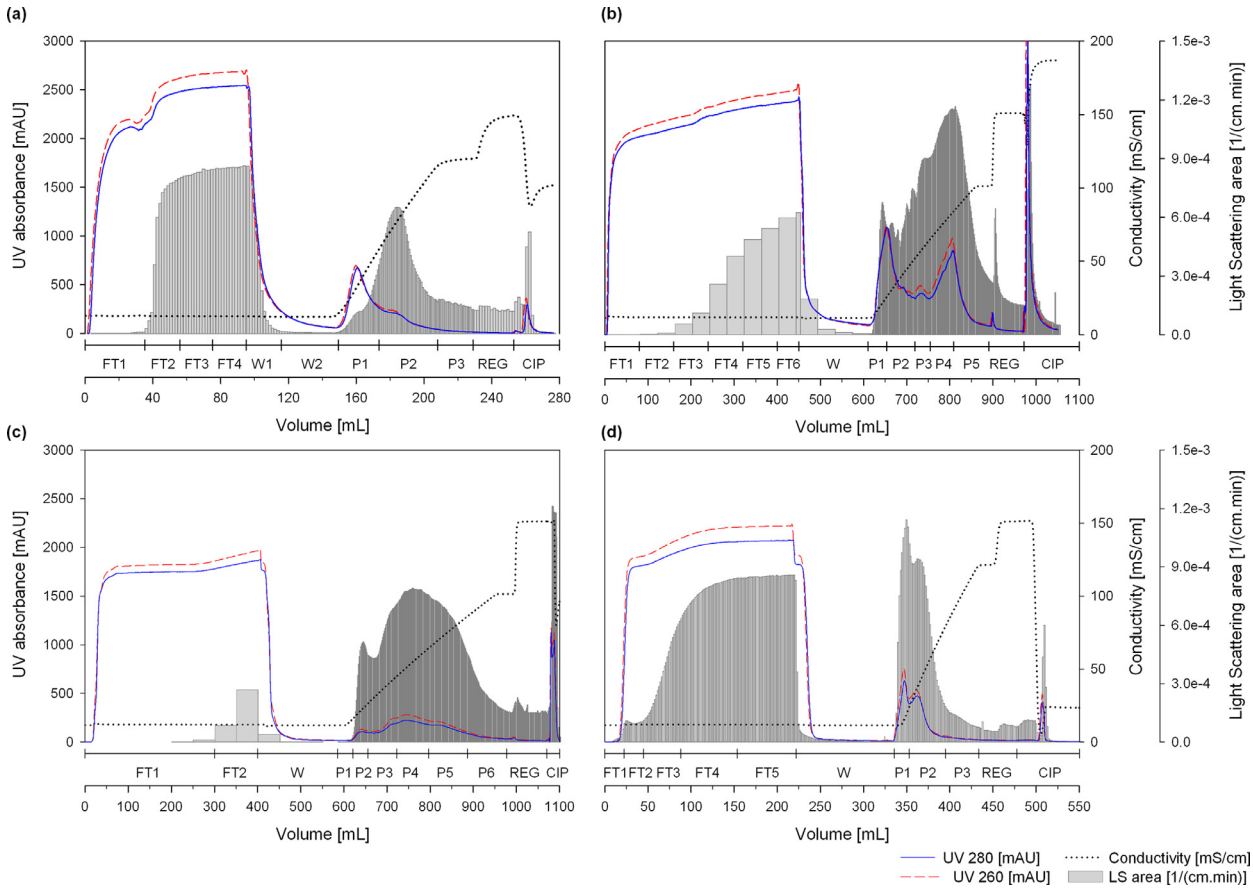

Fig. 2. Chromatograms of the capture and purification of HIV-1 gag VLPs using (a) NatriFlo® HD-Q Recon membrane adsorber, (b) CIMmultus™ QA-8 monolith, (c) Fractogel® EMD TMAE Hicap (M) column and (d) Capto™ Heparin column. FT: flow-through; W: wash; P: elution peaks; REG/2M: regeneration with 2 M NaCl; CIP: cleaning-in-place.

that led to less than 3% particle breakthrough in each one of the four tested strategies (measured by NTA, Table SA1-SA4). Taking this into account, the following capacities were estimated: Natrix-Membrane: 5.3 × 10^{12} particles/mL membrane (loading of 35 mL or 44 CV); QA-Monolith: 2.9 × 10^{12} particles/mL column (loading of 240 mL or 30 CV); Fractogel-TMAE: 1.5 × 10^{12} particles/mL column (loading of 400 mL or 17 CV) and Capto-Heparin: 1.5 × 10^{11} particles/mL column (loading of 45 mL or 2 CV). Anion-exchange based chromatography materials had the higher binding capacities for bionanoparticles. As expected, due their larger surface area accessible for binding of large molecules, membrane adsorber and monolith had slightly higher binding capacity than the porous-bead resin, in which bionanoparticles can only bind at the outer surface of the beads [8]. Nevertheless, all three materials had binding capacities in the same range (2-5 × 10^{12} particles/mL column or membrane) and the easy scalability of packed columns compensates for the lower binding capacity. The obtained values are also comparable to previously reported data [8,9,31]. For all three anion-exchangers a salt linear gradient was used as elution strategy (Table 2, Fig. 2).

3.3. Capture and purification of eVLPs using anion-exchange monoliths, membrane adsorbers and polymer-grafted porous beads

The membrane adsorber, Natrix-Membrane, showed the highest binding capacity and allowed the capture and semi-purification of HIV-1 gag VLPs directly from endonuclease treated and filtered CHO cell culture supernatant. At the beginning of the loading phase, while bionanoparticles bound to the membrane adsorber, part of the proteins and dsDNA flowed through the column (Fig. 2a, Table SA1: FT1). Bound proteins (P1) were separated from bound particles (P2) during the elution gradient. SDS-PAGE analysis (Fig 3a) shows a significant reduction in protein content from the loading material (L) to the elution fraction P2. This was confirmed by Bradford assay, in which the total protein content in P2 was lower than the lower limit of quantification (Table SA1). The presence of HIV-1 gag VLPs in P2 was confirmed by cryo-electron microscopy (Fig. 3d) in combination with the p24 Western blot assay (Fig. 3b) and proteomic analysis by mass spectrometry (Supplementary material B). However, co-elution of different particle populations was also observed by cryo-electron microscopy (Fig. 3d) and co-elution of dsDNA and chromatin was confirmed by Picogreen assay, H3-histone Western blot assay and proteomic analysis (Table SA1, Fig. 3c, Figure SA1, Supplementary material B). Nevertheless, a two-fold reduction in dsDNA content from the feed material to the fraction P2 was already achieved in a single step.

The QA-Monolith was also used for the direct capture of HIV-1 gag VLPs directly from endonuclease treated and filtered CHO cell culture supernatant (Fig. 2b). As for the Natrix-Membrane, at the beginning of loading phase of the QA-Monolith, part of the host cell proteins and dsDNA passed through the monolith while bionanoparticles bound (Table SA2). In contrast with the Natrix-Membrane, for the QA-Monolith, light scattering signal and NTA measurements revealed that particles elute across the entire elution gradient (Fig. 2b, Table SA2). Despite the presence of HIV-1 gag polyprotein was confirmed by p24 Western blot in all elution fractions (Fig. 4b), SDS-PAGE and proteomic analysis revealed that these different elution fractions (P1-P5) contained different

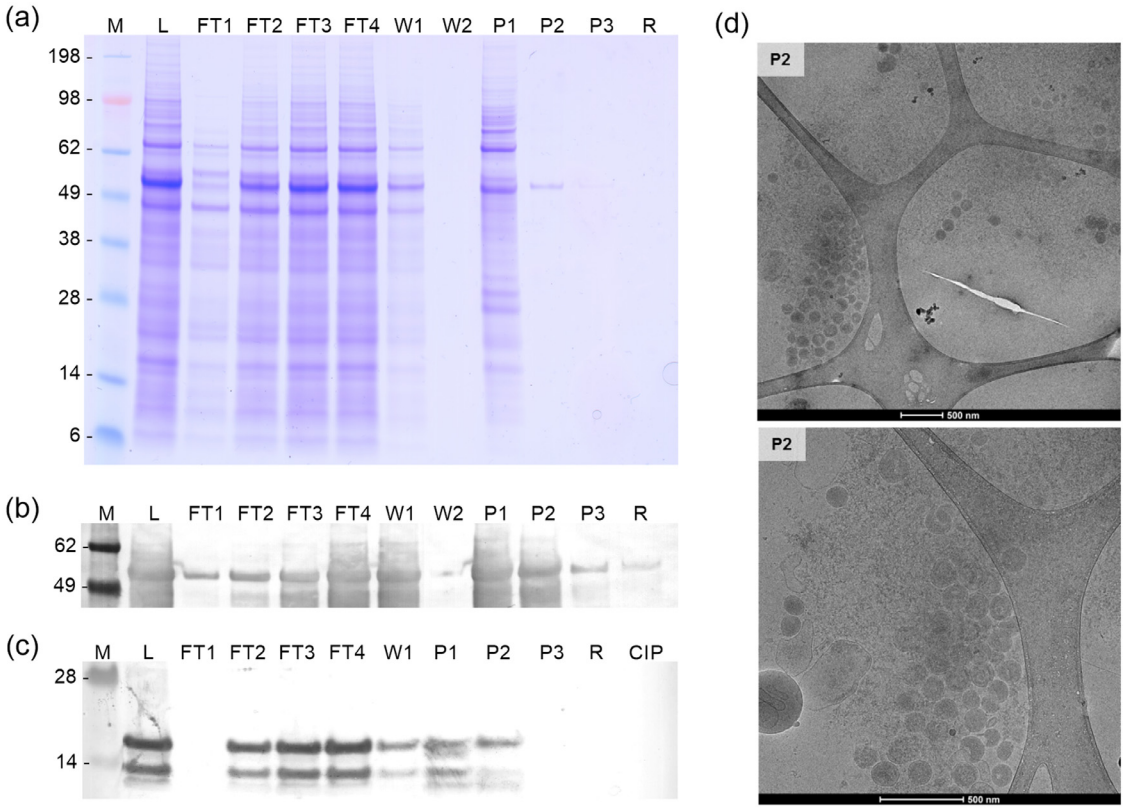

Fig. 3. SDS-PAGE (a), HIV-1 p24 (b) and H3-histone (c) Western blots and cryo-TEM micrographs (d) of relevant fractions from the capture and purification experiments using NatriFlo® HD-Q Recon membrane adsorber. M: molecular weight marker; FT: flow-through; W: wash; P: elution peaks; REG: regeneration with 2 M NaCl; CIP: cleaning-in-place.

proteins in their composition (Fig. 4a, Supplementary material B). Picogreen assay and H3-histone Westernblot showed that most of the bound dsDNA and chromatin eluted in fractions P2 and P3 (Table SA2, Fig. 4c). Cryo-electron micrographs showed the presence of HIV-1 gag VLPs in all elution fractions (Fig. 4d). Fractions P4 and P5 were considered the main product fractions due to the higher particle concentration and simultaneous lower total protein and dsDNA content per dose (hypothetical vaccination dose of 10^9 particles, Figure SA4). Despite that cryo-electron micrographs showed an enrichment of HIV-1 gag VLPs in fractions P4 and P5, some host cell derived bionanoparticles could still be found as well as disrupted VLPs (Fig. 4d). Additionally, according to H3-histone Western blot, proteomic analysis and Picogreen assay dsDNA and chromatin are still present in fractions P4 and P5 (Fig. 4c, Supplementary material B). Nevertheless, reductions of 13.3-fold for host cell protein and 2.9-fold for dsDNA, together with partial particle separation, were achieved using the QA-monolith. Capture and purification of HIV-1 gag VLPs directly from CHO cell culture supernatant using Fractogel^{-}TMAE was recently reported [8]. Due to the limited surface area available for binding of large molecules and aiming to increase the binding capacity for eVLPs, endonuclease treated and 0.8 µm filtered cell culture supernatant was pre-processed by flow-through chromatography using Capto-Core. Even though pre-processing of the feed material allowed a reduction of 73% of the total protein and 15% of dsDNA content (data not shown), the binding capacity increase was only 0.4-log. This strengthens the hypothesis that when using porous beads, small protein impurities bind to the ligands inside of the chromatography beads which are not accessible for VLPs, reducing the risk of binding competition or displacement effects. Similarly to the QA-Monolith, particle elution from the Fractogel-TMAE column occurred across the entire elution gradient (Fig. 2c, Table SA3). Moreover, according to SDS-PAGE and proteomic analysis, late elution fractions of QA-Monolith (P3-P5) and Fractogel-TMAE (P3-P6) contained similar proteins (Figs. 4 and 5 and Supplementary material B). Despite HIV-1 gag VLPs were identified in all elution fractions by cryo-electron microscopy (Fig. 5d), considering particle concentration together with the total protein and dsDNA per dose (Figure SA5) only fractions P5 and P6 were considered as main product fractions.

Pre-processing of cell culture supernatant using flow-through chromatography had the purpose of removing small impurities, mainly host cell proteins, and increase particle binding capacity. When using the membrane adsorber only 11% of the proteins bound to the membrane and were eluted before the particles at lower salt concentration (Table SA1). Similar behaviour was observed for the monolith, in which most of the bound proteins eluted also at lower salt concentration than most of the particles. Accordingly, no significant improvement on particle binding capacity would be expected, justifying the addition of another step in the process. Therefore, the strategy in which flow-through chromatography is placed before the membrane adsorber or monolith was not tested in this study.

3.4. Purification of eVLPs and removal of host cell derived bionanoparticles and chromatin using heparin-affinity chromatography

Purification of HIV-1 gag VLPs by heparin affinity was performed using Capto-Heparin. In order to remove potential heparin-binding host cell proteins, endonuclease treated and 0.8 µm filtered CHO cell culture supernatant was pre-processed by flow-through chromatography using Capto-Core as described in Section 3.1 (Figures SA1 and SA2).

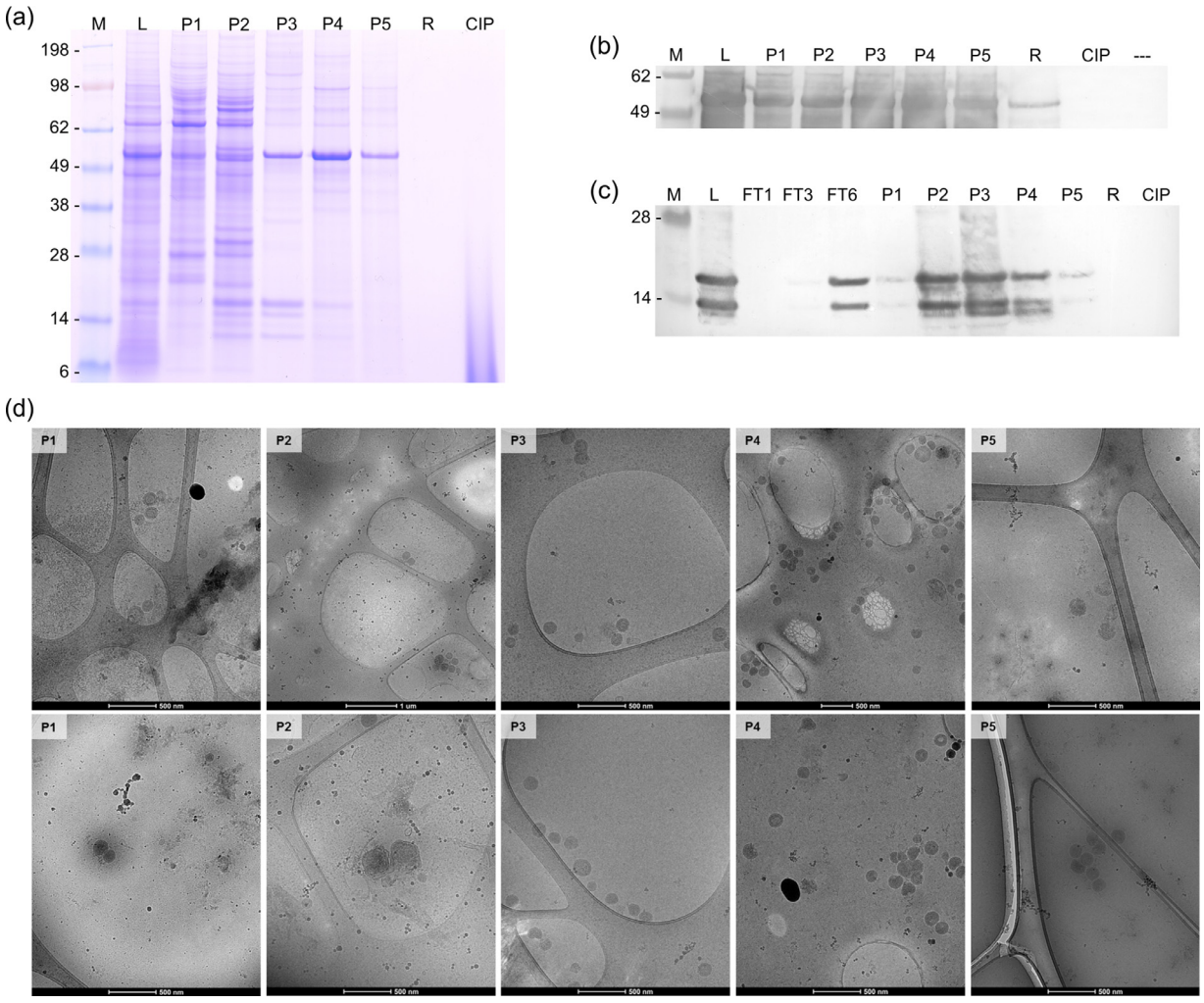

Fig. 4. SDS-PAGE (a), HIV-1 p24 (b) and H3-histone (c) Western blots and cryo-TEM micrographs (d) of relevant fractions from the capture and purification experiments using CIMmultus™ QA-8 monolith. M: molecular weight marker; FT: flow-through; W: wash; P: elution peaks; REG: regeneration with 2M NaCl; CIP: cleaning-in-place.

Contrarily to the anion-exchange based strategies, in which at the beginning of the loading phase all particles bound to the column/membrane, during the Capto-Heparin loading, particle breakthrough started immediately after the column void volume (light scattering signal, Fig. 2d). This indicates that, while some particles bound to the heparin ligands, others passed directly through the column. Similar behaviour was already reported for the purification HIV-1 gag VLPs produced in HEK 293 cells [22]. Cryo-electron micrographs showed that, despite of the presence of some HIV-1 gag VLPs, the majority of the particles eluting in the first flow-through fractions (FT2 and FT3) are host cell derived vesicles (Fig. 6d). Flow-through fractions FT4 and FT5 had a composition similar to the feed material indicating full breakthrough and column overloading (Table SA4, Figs. 1b and 6a-6d). Bound particles were eluted using a salt linear gradient (Table 2). Although no complete resolution was achieved, two elution peaks could be clearly distinguished, indicating the elution of different particle populations (Fig. 2d). SDS-PAGE and proteomic analysis showed that the protein composition of fractions P1 and P2 was different (Fig. 6a, Supplementary material B). Picogreen assay showed that fraction P2 contained 7 times more dsDNA than fraction P1 and proteomic analysis revealed that fraction P2 contained several histones while in P1 only histone H4 was found (Table SA4, Supplementary material B). Cryo-electron micrographs confirmed the different nature of the particles eluting in fractions P1 and P2 (Fig. 6d). Fraction P1 was enriched in HIV-1 gag VLPs, while fraction P2 contained mostly other particulate structures. Considering the identification of several histones by proteomic analysis, the high dsDNA content and the confirmation of the presence of H3-histone by Western blot analysis, the particulate structures in fraction P2 were identified as chromatin, a complex of host cell proteins and DNA. This was additionally confirmed by immunogold labelling of H3-histones and negative staining TEM (data not shown). Moreover, similar structures were previously reported in cryo-electron micrographs as chromatin [32]. These results additionally explain recoveries of more than 100% for dsDNA in chromatographic experiments which use salt to promote elution. The disruption of the chromatin complexes due to the higher salt concentrations during elution results in the release of dsDNA enabling its quantification. It is important to note than in both fractions, P1 and P2, nearly the same number of particles were quantified by NTA (Table SA4) and an average diameter of approximately 150 nm was measured also for both. These results clearly show the need for combining several biophysical, biochemical and high-resolution imaging methods for the quantification and characterization of eVLPs. Moreover, these results show that with the available methodologies specific quantification of eVLPs in complex mixtures such as cell culture supernatants is very difficult and impossible without advanced methodology.

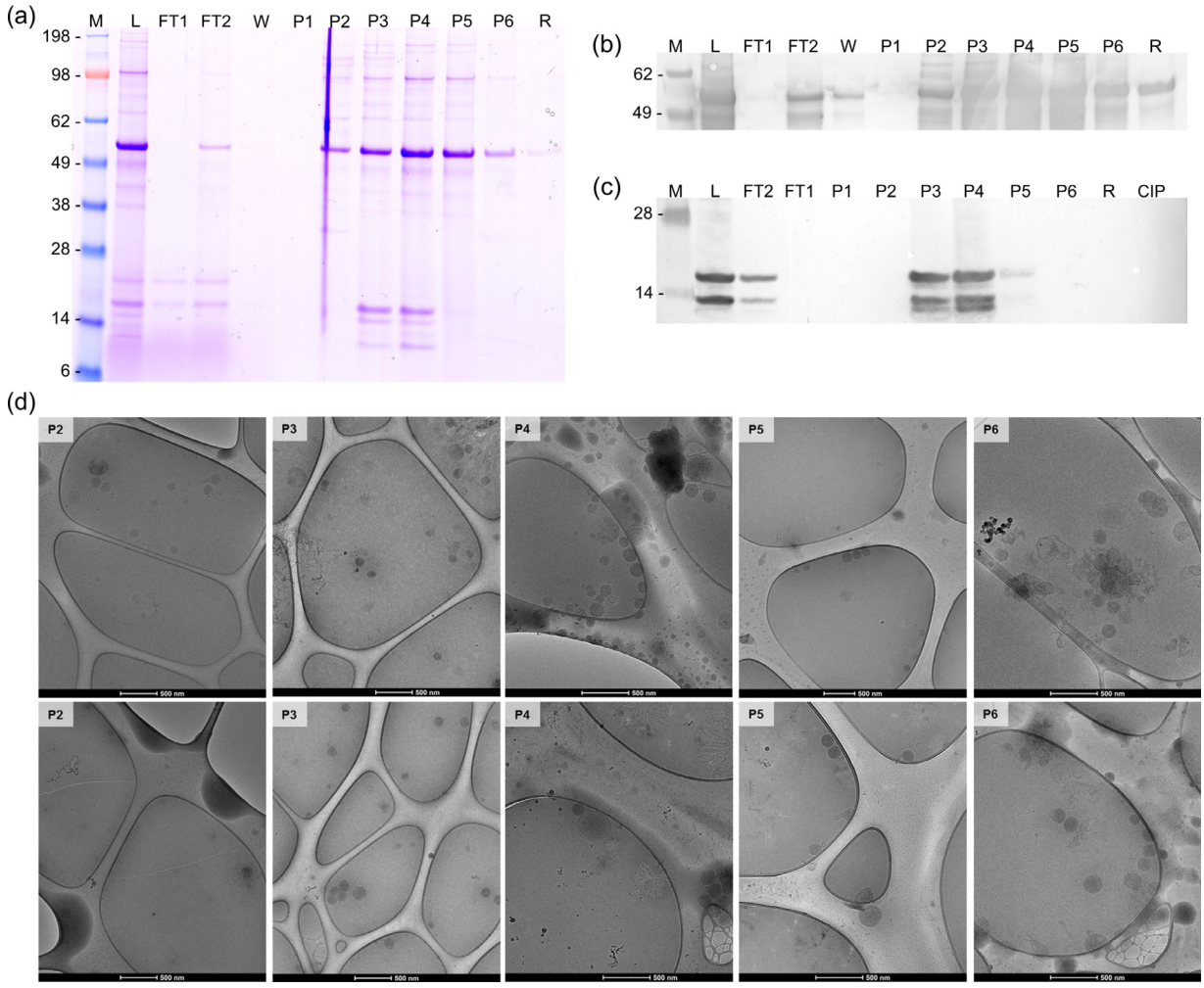

Fig. 5. SDS-PAGE (a), HIV-1 p24 (b) and H3-histone (c) Western blots and cryo-TEM micrographs (d) of relevant fractions from the capture and purification experiments using Fractogel® EMD TMAE Hicap (M). M: molecular weight marker; FT: flow-through; W: wash; P: elution peaks; REG: regeneration with 2M NaCl; CIP: cleaning-in-place.

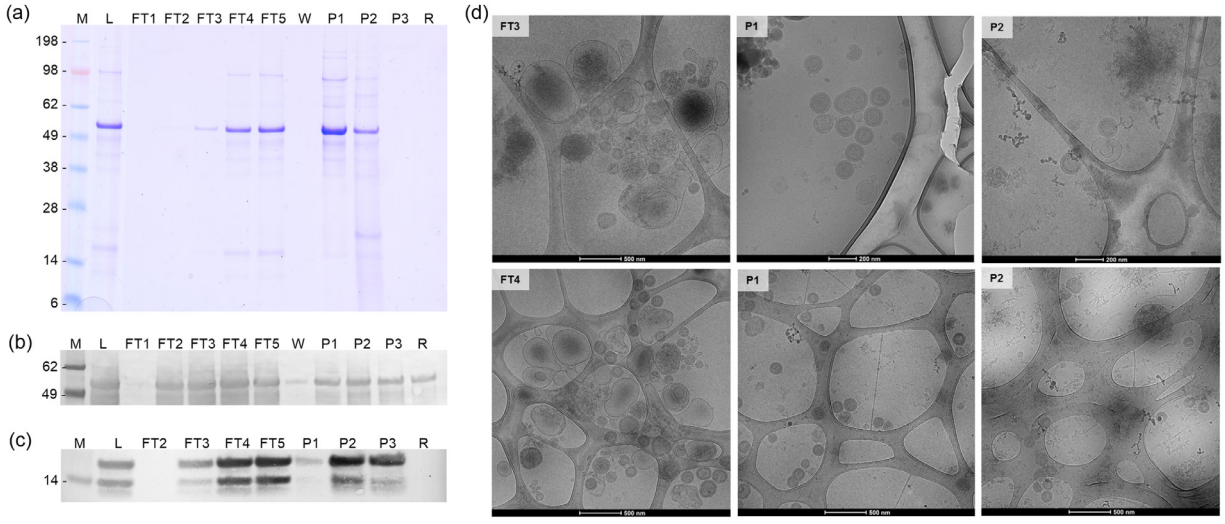

Fig. 6. : SDS-PAGE (a), HIV-1 p24 (b) and H3-histone (c) Western blots and cryo-TEM micrographs (d) of relevant fractions from the capture and purification experiments using Capto™ Heparin. M: molecular weight marker; FT: flow-through; W: wash; P: elution peaks; REG: regeneration with 2 M NaCl; CIP: cleaning-in-place.

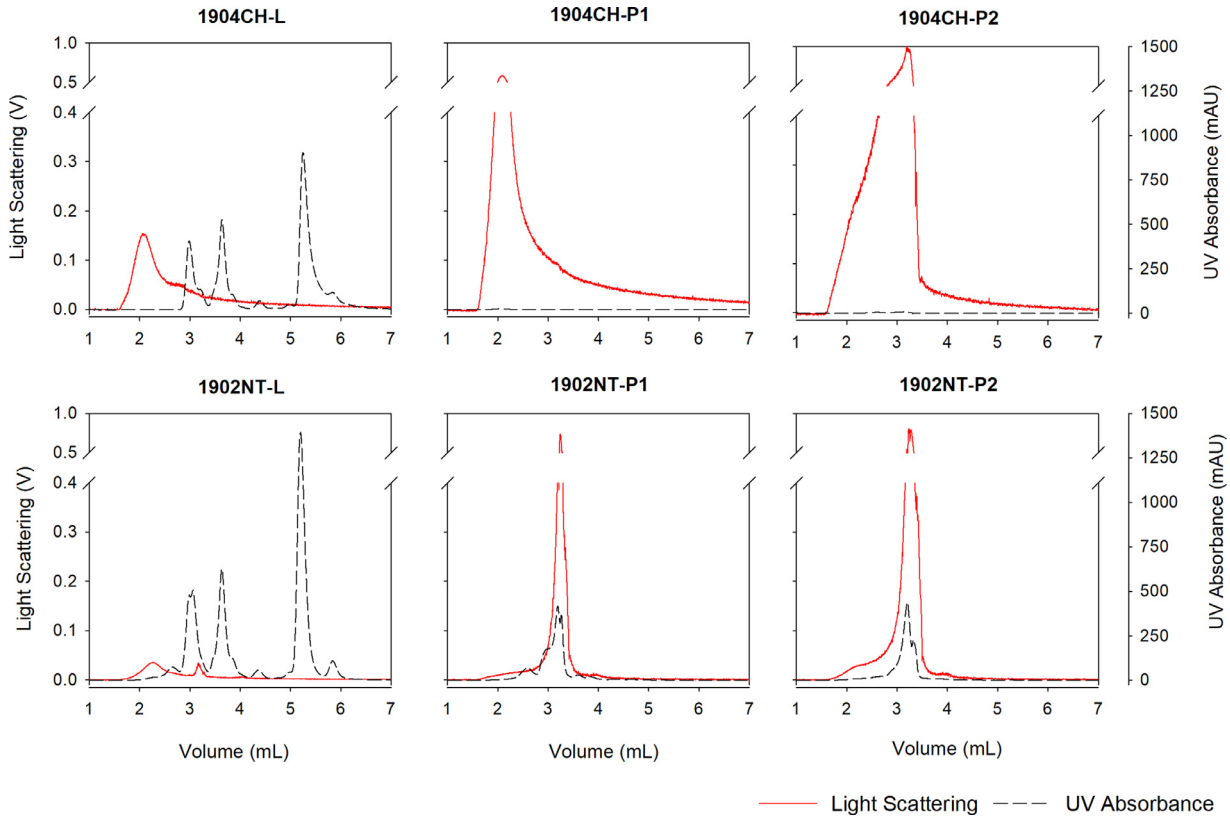

Fig. 7. Chromatograms of analytical size exclusion chromatography experiments of relevant fractions from the capture and purification experiments using NatriFlo® HD-Q Recon membrane adsorber (1902NT) and Capto™ Heparin (1904CH). Light scattering signal: 90° angle detector; UV absorbance at 280 nm. L: loading material; P: elution peaks.

3.5. Purity and recovery of main product fractions

Size exclusion analytical chromatography coupled to multi-angle light scattering (SEC-MALS) was used to semi-quantitatively access the purity of all elution fractions (Figure SA7). As an example, SEC-MALS chromatograms of relevant fractions from the DSP strategy with higher binding capacity (Natrix-Membrane: 1902NT) and the DSP strategy with better bionanoparticle separation (Capto-Heparin: 1904CH) are shown in Fig. 7. In all tested DSP strategies, significant reduction of UV absorbance signal of impurities (eluting from approximately 2.5 to 6 mL) could be observed from the feed material to the main product fractions, indicating an increase in purity. As discussed in Section 3.4, in the Capto-Heparin experiment, fraction P1 contained mainly HIV-1 gag VLPs while fraction P2 contained mainly chromatin. SEC-MALS chromatogram of fraction P1 showed that HIV-1 gag VLPs elute in the void volume of the SEC column (light scattering signal starting at approximately 1.5 mL and with peak maximum at 2.1 mL). SEC-MALS chromatogram of fraction P2 (chromatin rich fraction) showed that despite particle elution (light scattering signal) also started at approximately 1.5 mL, the peak maximum was shifted to approximately 3.2 mL indicating the elution of smaller molecules or particle retention by interaction with the SEC column. Interestingly, this was not observed in the SEC-MALS chromatograms of the feed material or flow-through fractions. The reason for that is that chromatin structure is disrupted at moderate-high salt concentrations

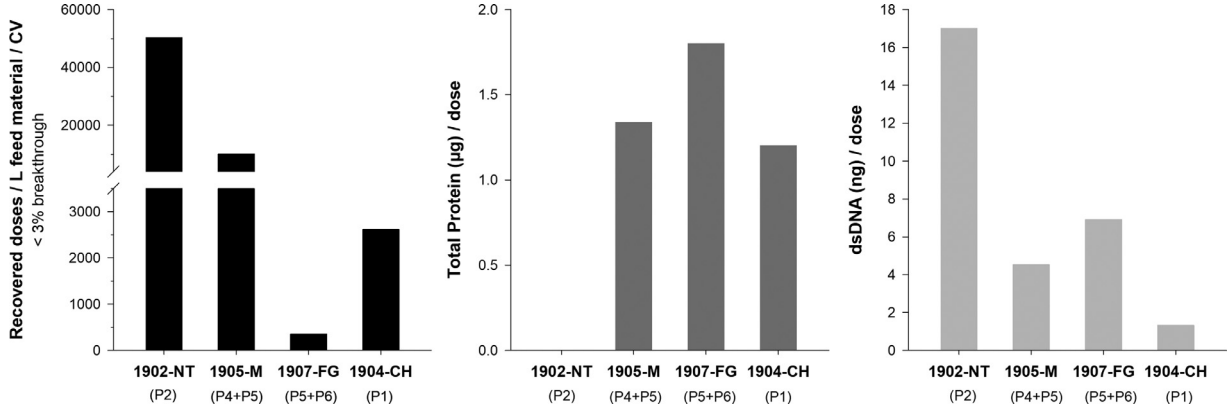

Fig. 8. Comparison of recovered doses per litre of cell culture supernatant, total protein per dose and dsDNA per dose in the main product fractions. 1902-NT: NatriFlo® HD-Q Recon membrane adsorber; 1905-M: CIMmultus™ QA-8 monolith; 1907-FG: Fractogel® EMD TMAE Hicap (M); 1904-CH: Capto™ Heparin.

[33] as the ones used during elution, resulting in smaller and more flexible structures that are longer retained in the SEC column.

Specific quantification of HIV-1 gag VLPs in the feed material by particle quantification methods, such as NTA or SEC-MALS, was not possible due to the presence of other particulate structures such as host cell derived bionanoparticles and chromatin. Likewise, HIV-1 gag VLP concentration could not be estimated by quantifying the HIV-1 gag polyprotein due to the presence of free HIV-1 gag protein in solution which was produced by the cells but did not assemble into VLPs. Consequently, direct determination of the yield of HIV-1 gag VLPs was not possible. In order to compare the performance of the tested DSP strategies for the capture and purification of HIV-1 gag VLPs we determined the recovered doses in the main product fractions considering a hypothetical vaccination dose of 10^9 particles (Fig. 8) under the assumption that particles in this main fraction are exclusively product. Additionally, we normalized the calculated recoveries considering the volume of feed material loaded in each experiment before 3% particle breakthrough was reached and considering the column/membrane volume. This product yield can only serve as an estimate due to the lack of proper analytics, but as TEM micrographs show that the main component in all selected product peaks is indeed intact VLP attributing the whole particle fraction of those peaks to being product is justified. Taking this into account, convective media (membrane adsorber and monolith) allowed the recovery of higher number of doses than the porous-bead resins. Nevertheless, scalability of bead-based resins easily overcomes the lower recovery as monolithic columns and membrane adsorbers are currently restricted to a couple of litres. For assessment and comparison of the purity of the main product fractions, total protein and dsDNA contents were normalized by the number of recovered doses (Fig. 8). Natrix-Membrane had the highest recovery, however HIV-1 gag VLPs could not be separated from host cell derived bionanoparticles. Highest overall purity was achieved using Capto-Heparin which allowed not only the separation of HIV-1 gag VLPs from host cell derived bionanoparticles but also the separation of VLPs from chromatin. Polymer-grafted beads (Fractogel-TMAE) and monoliths (QA-Monolith) main product fractions had similar final composition. Despite QA-Monolith had a significantly higher recovery than Fractogel-TMAE, packed beads can be easily scaled up to hundreds of litres while monoliths have been successfully scaled up only up to 8 L.

4. Conclusion

Anion-exchange chromatography is suitable for capture and semi-purification of enveloped VLPs directly from cell culture supernatant. A fast capture of HIV-1 gag VLPs directly from endonuclease-treated and filtered CHO cell culture supernatant was possible using the membrane adsorber, NatriFlo® HD-Q Recon. Heparin-affinity chromatography is suitable for purification of eVLPs as well. Capto™ Heparin allowed the separation of HIV-1 gag VLPs from host cell derived bionanoparticles and chromatin. The best performer including factors like scalability, removal of host cell bionanoparticles, protein and dsDNA was the strategy combining flow-through chromatography using Capto™ Core 700 and Heparin-affinity chromatography using Capto™ Heparin. Regardless of the significant recent advances in eVLP DSP, development and optimization are still severely hindered by the lack of high-resolution methodologies for eVLP detection and quantification in complex mixtures, especially due to the presence of host cell derived bionanoparticles and chromatin. While we successfully showed the use of cryo-electron micrographs for particle identification, this methodology is not suited for rapid process development and significant amounts of highly pure eVLPs are required to allow the development and validation of novel analytical technologies. At the same time, to obtain highly pure eVLPs, DSP development and optimization are required. Therefore, a simultaneous development and optimization of both DSP and analytical technologies is essential in the future.

Declaration of competing interest

The authors declare that they have no known competing financial interests or personal relationships that could have appeared to influence the work reported in this paper.

CRediT authorship contribution statement

Patricia Pereira Aguilar: Data curation, Formal analysis, Investigation, Methodology, Project administration, Visualization, Writing - original draft, Writing - review & editing. **Katrin Reiter:** Formal analysis, Investigation. **Viktoria Wetter:** Formal analysis, Investigation. **Petra Steppert:** Supervision. **Daniel Maresch:** Data curation, Formal analysis, Investigation, Methodology, Resources. **Wai Li Ling:** Investigation, Methodology, Resources. **Peter Satzer:** Project administration, Supervision, Writing - review & editing. **Alois Jungbauer:** Funding acquisition, Project administration, Resources, Supervision, Writing - review & editing.

Acknowledgements

This project has been supported by the Austrian Science Fund (project BioToP; FWF W1224). Reiter and Wetter have been supported by the Austrian BMWD, BMVIT, SFG, Standortagentur Tirol, Government of Lower Austria and Business Agency Vienna through the Austrian FFG-COMET-Funding Program. This work used the platforms of the Grenoble Instruct-ERIC Centre (ISBG; UMS 3518 CNRS-CEA-UGA-EMBL) with support from FRISBI (ANR-10-INSB-05-02) and GRAL (ANR-10-LABX-49-01) within the Grenoble Partnership for Structural Biology (PSB). The IBS electron microscope facility is supported by the Auvergne-Rhône-Alpes Region, the Fonds FEDER, the Fondation Recherche Médicale (FRM), and the GIS-Infrastructures en Biologie Santé et Agronomie (IBISA). IBS acknowledges integration into the Interdisciplinary Research Institute of Grenoble (IRIG, CEA). The funding agencies had no influence on the conduct of this research.

Additionally the authors would like to acknowledge Icosagen (Tartumaa, Estonia) for producing the HIV-1 gag VLPs and providing the cell culture supernatant.

Supplementary materials

Supplementary material associated with this article can be found, in the online version, at doi:10.1016/j.chroma.2020.461378.

References

[1] S.H. Wong, A. Jassey, J.Y. Wang, W.C. Wang, C.H. Liu, L.T. Lin, Virus-like particle systems for vaccine development against viruses in the flaviviridae family, Vaccines (2019) 7.
[2] L. Cervera, F. Gòdia, F. Tarrés-Freixas, C. Aguilar-Gurrieri, J. Carrillo, J. Blanco, S. Gutiérrez-Granados, Production of HIV-1-based virus-like particles for vaccination: achievements and limits, Appl. Microbiol. Biotechnol. 103 (2019) 7367–7384.
[3] M.O. Mohsen, L. Zha, G. Cabral-Miranda, M.F. Bachmann, Major findings and recent advances in virus–like particle (VLP)-based vaccines, Semin. Immunol. 34 (2017) 123–132.
[4] M. Zhao, M. Vandersluis, J. Stout, U. Haupts, M. Sanders, R. Jacquemart, Affinity chromatography for vaccines manufacturing: finally ready for prime time? Vaccine 37 (2019) 5491–5503.
[5] T. Vicente, A. Roldão, C. Peixoto, M.J.T. Carrondo, P.M. Alves, Large-scale production and purification of VLP-based vaccines, J. Invert. Pathol. 107 (2011) S42–S48.
[6] P. Nestola, C. Peixoto, R.R.J.S. Silva, P.M. Alves, J.P.B. Mota, M.J.T. Carrondo, Improved virus purification processes for vaccines and gene therapy, Biotechnol. Bioeng. 112 (2015) 843–857.

[7] L.H. Lua, N.K. Connors, F. Sainsbury, Y.P. Chuan, N. Wibowo, A.P. Middelberg, Bioengineering virus-like particles as vaccines, Biotechnol. Bioeng. 111 (2014) 425–440.
[8] P. Pereira Aguilar, T.A. Schneider, V. Wetter, D. Maresch, W.L. Ling, A. Tover, P. Steppert, A. Jungbauer, Polymer-grafted chromatography media for the purification of enveloped virus-like particles, exemplified with HIV-1 gag VLP, Vaccine 37 (2019) 7070–7080.
[9] P. Steppert, D. Burgstaller, M. Klausberger, E. Berger, P.P. Aguilar, T.A. Schneider, P. Kramberger, A. Tover, K. Nobauer, E. Razzazi-Fazeli, A. Jungbauer, Purification of HIV-1 gag virus-like particles and separation of other extracellular particles, J. Chromatogr. A 1455 (2016) 93–101.
[10] Z. Kimia, S.N. Hosseini, S.S. Ashraf Talesh, M. Khatami, A. Kavianpour, A. Javidanbardan, A novel application of ion exchange chromatography in recombinant hepatitis B vaccine downstream processing: improving recombinant HBsAg homogeneity by removing associated aggregates, J. Chromatogr. B 1113 (2019) 20–29.
[11] L.M. Fischer, M.W. Wolff, U. Reichl, Purification of cell culture-derived influenza A virus via continuous anion exchange chromatography on monoliths, Vaccine 36 (2018) 3153–3160.
[12] G. Carta, A. Jungbauer, Protein Chromatography: Process Development and Scale-Up, Wiley-VHC Verlag GmbH & Co. KGaA, Weinheim, 2010.
[13] A. Zöchling, R. Hahn, K. Ahrer, J. Urthaler, A. Jungbauer, Mass transfer characteristics of plasmids in monoliths, J. Sep. Sci. 27 (2004) 819–827.
[14] R. Ghosh, Protein separation using membrane chromatography: opportunities and challenges, J. Chromatogr. A 952 (2002) 13–27.
[15] M. Krajacic, M. Ravnikar, A. Štrancar, I. Gutiérrez-Aguirre, Application of monolithic chromatographic supports in virus research, Electrophoresis 38 (2017) 2827–2836.
[16] M. Banjac, E. Roethl, F. Gelhart, P. Kramberger, B.L. Jarc, M. Jarc, A. Štrancar, T. Muster, M. Peterka, Purification of Vero cell derived live replication deficient influenza A and B virus by ion exchange monolith chromatography, Vaccine 32 (2014) 2487–2492.
[17] P. Gerster, E.-M. Kopecky, N. Hammerschmidt, M. Klausberger, F. Krammer, R. Grabherr, C. Mersich, L. Urbas, P. Kramberger, T. Paril, M. Schreiner, K. Nöbauer, E. Razzazi-Fazeli, A. Jungbauer, Purification of infective baculoviruses by monoliths, J. Chromatogr. A 1290 (2013) 36–45.
[18] K. Zimmermann, O. Scheibe, A. Kocourek, J. Muelich, E. Jurkiewicz, A. Pfeifer, Highly efficient concentration of lenti- and retroviral vector preparations by membrane adsorbers and ultrafiltration, BMC Biotechnol. 11 (2011) 55.
[19] B. Kalbfuss, M. Wolff, L. Geisler, A. Tappe, R. Wickramasinghe, V. Thom, U. Reichl, Direct capture of influenza A virus from cell culture supernatant with Sartobind anion-exchange membrane adsorbers, J. Membr. Sci. 299 (2007) 251–260.
[20] T.A. Grein, R. Michalsky, M. Vega López, P. Czermak, Purification of a recombinant baculovirus of Autographa californica M nucleopolyhedrovirus by ion exchange membrane chromatography, J. Virol. Methods 183 (2012) 117–124.
[21] M. de las Mercedes Segura, A. Kamen, A. Garnier, Purification of retrovirus particles using heparin affinity chromatography, in: J.M.Le Doux (Ed.), Gene Therapy Protocols: Design and Characterization of Gene Transfer Vectors, Humana Press, Totowa, NJ, 2008, pp. 1–11.
[22] K. Reiter, P.P. Aguilar, V. Wetter, P. Steppert, A. Tover, A. Jungbauer, Separation of virus-like particles and extracellular vesicles by flow-through and heparin affinity chromatography, J. Chromatogr. A 1588 (2019) 77–84.
[23] N. An, P. Gong, H. Hou, W. Chi, H. Jin, L. Zhao, Q. Tan, X. Tang, F. Wang, H. Jin, R. Zhang, Fabrication of macroporous microspheres with core-shell structure for negative chromatography purification of virus, J. Chromatogr. A (2019) 460578.
[24] K.T. James, B. Cooney, K. Agopsowicz, M.A. Trevors, A. Mohamed, D. Stoltz, M. Hitt, M. Shmulevitz, Novel high-throughput approach for purification of infectious virions, Sci. Rep. 6 (2016) 36826.
[25] X. Ding, D. Liu, G. Booth, W. Gao, Y. Lu, Virus-like particle engineering: from rational design to versatile applications, Biotechnol. J. 13 (2018) 1700324.
[26] S.B. Carvalho, R.J.S. Silva, M.G. Moleirinho, B. Cunha, A.S. Moreira, A. Xenopoulos, P.M. Alves, M.J.T. Carrondo, C. Peixoto, Membrane-based approach for the downstream processing of influenza virus-like particles, Biotechnol. J. 14 (2019) e1800570.
[27] M.W. Wolf, U. Reichl, Downstream processing of cell culture-derived virus particles, Expert Rev. Vaccines 10 (2011) 1451–1475.
[28] E. Nolte-'t Hoen, T. Cremer, R.C. Gallo, L.B. Margolis, Extracellular vesicles and viruses: are they close relatives? Proc. Natl. Acad. Sci. U.S.A. 113 (2016) 9155–9161.
[29] B. Michen, T. Graule, Isoelectric points of viruses, J. Appl. Microbiol. 109 (2010) 388–397.
[30] P. Pereira Aguilar, I. Gonzalez-Dominguez, T.A. Schneider, F. Godia, L. Cervera, A. Jungbauer, At-line multi-angle light scattering detector for faster process development in enveloped virus-like particle purification, J. Sep. Sci. 42 (2019) 2640–2649.
[31] T. Vicente, C. Peixoto, M.J. Carrondo, P.M. Alves, Purification of recombinant baculoviruses for gene therapy using membrane processes, Gene. Ther. 16 (2009) 766–775.
[32] Q. Fang, P. Chen, M. Wang, J. Fang, N. Yang, G. Li, R.M. Xu, Human cytomegalovirus IE1 protein alters the higher-order chromatin structure by targeting the acidic patch of the nucleosome, Elife 5 (2016).
[33] A. Gansen, J. Langowski, Nucleosome dynamics studied by förster resonance energy transfer, in: D.P. Bazett-Jones, G. Dellaire (Eds.), The Functional Nucleus, Springer International Publishing, Cham, 2016, pp. 329–356.